



RESEARCH ARTICLE

Rescue of DNA-PK Signaling and T-Cell Differentiation by Targeted Genome Editing in a *prkdc* Deficient iPSC Disease Model

Shamim H. Rahman^{1,2,3}, Johannes Kuehle³, Christian Reimann^{1,2},
Tafadzwa Mlambo^{1,2,4}, Jamal Alzubi^{1,2,3}, Morgan L. Maeder^{5,6}, Heimo Riedel^{3,7},
Paul Fisch⁸, Tobias Cantz⁹, Cornelia Rudolph¹⁰, Claudio Mussolino^{1,2}, J. Keith Joung^{5,6},
Axel Schambach^{3†*}, Toni Cathomen^{1,2,3†*}

1 Institute for Cell and Gene Therapy, University Medical Center Freiburg, Freiburg, Germany, **2** Center for Chronic Immunodeficiency, University Medical Center Freiburg, Freiburg, Germany, **3** Institute of Experimental Hematology, Hannover Medical School, Hannover, Germany, **4** Spemann Graduate School of Biology and Medicine (SGBM), University of Freiburg, Freiburg, Germany, **5** Molecular Pathology Unit, Massachusetts General Hospital, Charlestown, Massachusetts, United States of America, **6** Department of Pathology, Harvard Medical School, Boston, Massachusetts, United States of America, **7** Department of Biochemistry and Mary Babb Randolph Cancer Center, Robert C. Byrd Health Sciences Center, West Virginia University, Morgantown, West Virginia, United States of America, **8** Institute of Pathology, University Medical Center Freiburg, Freiburg, Germany, **9** Translational Hepatology and Stem Cell Biology, REBIRTH cluster of excellence, Hannover Medical School, Hannover, Germany, **10** Institute for Cellular and Molecular Pathology, Hannover Medical School, Hannover, Germany

 These authors contributed equally to this work.

† AS and TC also contributed equally to this work.

* Schambach.Axel@mh-hannover.de (AS); Toni.Cathomen@uniklinik-freiburg.de (TC)



click for updates

 OPEN ACCESS

Citation: Rahman SH, Kuehle J, Reimann C, Mlambo T, Alzubi J, Maeder ML, et al. (2015) Rescue of DNA-PK Signaling and T-Cell Differentiation by Targeted Genome Editing in a *prkdc* Deficient iPSC Disease Model. *PLoS Genet* 11(5): e1005239. doi:10.1371/journal.pgen.1005239

Editor: Derry C. Roopenian, The Jackson Laboratory, UNITED STATES

Received: November 3, 2014

Accepted: April 26, 2015

Published: May 22, 2015

Copyright: © 2015 Rahman et al. This is an open access article distributed under the terms of the [Creative Commons Attribution License](https://creativecommons.org/licenses/by/4.0/), which permits unrestricted use, distribution, and reproduction in any medium, provided the original author and source are credited.

Data Availability Statement: All relevant data are within the paper and its Supporting Information files.

Funding: This work was supported by the German Research Foundation [SPP1230Ca311/2 to TCat; SFB 738C9 to AS and TCat; the REBIRTH Cluster of Excellence to AS and TCat (EXC 62/1) and JA and JK (fellowships)], the German Federal Ministry of Education and Research [BMBF 01E00803 to TCat; ReGene-01GN1003D to TCat and AS], the German Academic Exchange Service [DAAD fellowship to TM], the European Commission's 7th Framework Program [PERSIST-222878 to TCat], the National

Abstract

In vitro disease modeling based on induced pluripotent stem cells (iPSCs) provides a powerful system to study cellular pathophysiology, especially in combination with targeted genome editing and protocols to differentiate iPSCs into affected cell types. In this study, we established zinc-finger nuclease-mediated genome editing in primary fibroblasts and iPSCs generated from a mouse model for radiosensitive severe combined immunodeficiency (RS-SCID), a rare disorder characterized by cellular sensitivity to radiation and the absence of lymphocytes due to impaired DNA-dependent protein kinase (DNA-PK) activity. Our results demonstrate that gene editing in RS-SCID fibroblasts rescued DNA-PK dependent signaling to overcome radiosensitivity. Furthermore, *in vitro* T-cell differentiation from iPSCs was employed to model the stage-specific T-cell maturation block induced by the disease causing mutation. Genetic correction of the RS-SCID iPSCs restored T-lymphocyte maturation, polyclonal V(D)J recombination of the T-cell receptor followed by successful beta-selection. In conclusion, we provide proof that iPSC-based *in vitro* T-cell differentiation is a valuable paradigm for SCID disease modeling, which can be utilized to investigate disorders of T-cell development and to validate gene therapy strategies for T-cell deficiencies. Moreover, this study emphasizes the significance of designer nucleases as a tool for generating isogenic disease models and their future role in producing autologous, genetically corrected transplants for various clinical applications.

Institutes of Health [R01 GM088040 to JKJ], and the National Science Foundation [Graduate Research Fellowship to MLM]. The funders had no role in study design, data collection and analysis, decision to publish, or preparation of the manuscript.

Competing Interests: TCat is a consultant for TRACR Hematology Ltd. JKJ is a consultant for Horizon Discovery. JKJ has financial interests in Editas Medicine, Hera Testing Laboratories, Poseida Therapeutics, and Transposagen Biopharmaceuticals. JKJ's interests were reviewed and are managed by Massachusetts General Hospital and Partners HealthCare in accordance with their conflict of interest policies. Following the completion of her work for this project, MLM has become an employee of Editas Medicine.

Author Summary

Due to the limited availability and lifespan of some primary cells, *in vitro* disease modeling with induced pluripotent stem cells (iPSCs) offers a valuable complementation to *in vivo* studies. The goal of our study was to establish an *in vitro* disease model for severe combined immunodeficiency (SCID), a group of inherited disorders of the immune system characterized by the lack of T-lymphocytes. To this end, we generated iPSCs from fibroblasts of a radiosensitive SCID (RS-SCID) mouse model and established a protocol to recapitulate T-lymphopoiesis from iPSCs *in vitro*. We used designer nucleases to edit the underlying mutation in *prkdc*, the gene encoding DNA-PKcs, and demonstrated that genetic correction of the disease locus rescued DNA-PK dependent signaling, restored normal radiosensitivity, and enabled T-cell maturation and polyclonal T-cell receptor recombination. We hence provide proof that the combination of two promising technology platforms, iPSCs and designer nucleases, with a protocol to generate T-cells *in vitro*, represents a powerful paradigm for SCID disease modeling and the evaluation of therapeutic gene editing strategies. Furthermore, our system provides a basis for further development of iPSC-derived cell products with the potential for various clinical applications, including infusions of *in vitro* derived autologous T-cells to stabilize patients after hematopoietic stem cell transplantation.

Introduction

Studying the molecular pathology of human disease is often difficult due to the limited availability of particular primary cells, their limited lifespan, or because complex developmental differentiation procedures cannot be easily followed *in vivo*. *In vitro* disease modeling with induced pluripotent stem cells (iPSCs) provides a practical alternative, and the study of several disorders has benefitted enormously from the convergence of three key technologies: modern genomics that links genetic variants to disease phenotypes, the ability to generate patient-specific iPSCs that can be differentiated into cell types affected by disease, and powerful tools for editing complex genomes [1,2].

T lymphocytes play an important role in adaptive immunity against invading pathogens or in fighting tumor cells. A natural microenvironment for T-cell lymphopoiesis is provided by the thymus. Inherited defects in T-cell function or in T-cell development can lead to severe combined immunodeficiency (SCID), a group of life threatening disorders of the immune system [3]. Radiosensitive SCID (RS-SCID; OMIM #602450) is characterized on the molecular level by dysfunctional non-homologous end-joining (NHEJ), the most important pathway to repair DNA double strand breaks (DSBs). In human patients, defective DNA repair can lead to a cellular hypersensitivity to ionizing radiation. Moreover NHEJ is essential for physiological B- and T-lymphocyte development as it plays an important role in the B-cell receptor (BCR) and T-cell receptor (TCR) recombination process [4]. The diversity of BCRs and TCRs results from the multitude of variable (V), divers (D) and joining (J) gene segments that are almost randomly reassembled in a process called V(D)J recombination. During V(D)J recombination, specific enzymes cleave at specific recombination signal sequences flanking these gene segments and NHEJ factors play a crucial role in reassembly and final ligation of these gene segments [5,6]. The NHEJ process involves a number of different enzymes, including DNA-dependent protein kinase (DNA-PK). DNA-PK is a polyprotein complex, formed by the Ku70/Ku80 heterodimer and the DNA-PK catalytic subunit (DNA-PKcs) [7], that binds to DNA end structures and serves as a docking site for additional NHEJ factors that mediate DNA repair

[8]. Hypomorphic mutations in *PRKDC*, the locus encoding DNA-PKcs, have recently been described for radiosensitive T and B deficient SCID patients [9]. Hence, DNA-PK dependent signaling is a paradigmatic example of how a single molecule can be simultaneously involved in both, DNA repair and T- and B-cell development, and of how such a process can be disturbed by a single point mutation. These particularities make *PRKDC* an optimal target for novel site-specific gene therapy approaches, such as designer nuclease mediated genome editing.

For disease modeling, iPSCs can be generated from affected somatic cells by expression of four transcription factors Oct4, Sox2, Klf4 and c-Myc [10,11]. Similar to pluripotent embryonic stem cells, iPSCs have the capacity for unlimited self-renewal, are permissive for transfection with foreign DNA, and importantly, can be expanded in a clonal fashion for characterization. Thus far, iPSCs have been derived from several patients suffering from different hematopoietic and immunological disorders and have been used for disease modeling and gene targeting approaches [12]. Several protocols for *in vitro* [13–21] and *in vivo* [22,23] differentiation of iPSCs to hematopoietic cells have been reported. The availability of Notch ligand based cell culture systems, such as the murine stromal cell line OP9-DL1, allows for further differentiation of hematopoietic stem cells into T-cells *in vitro* [24,25].

Targeted genome modification in iPSCs is an essential tool in disease modeling [12], and gene editing with designer nucleases has developed into a powerful instrument, which has been successfully applied to generate various genetically modified model organisms or human cells to study gene function or the pathophysiology of disease causing mutations. Designer nucleases, like meganucleases [26], zinc-finger nucleases (ZFNs) [27], transcription activator-like effector nucleases (TALEN) [28], or the clustered regularly interspaced short palindromic repeats (CRISPR)/Cas9 system [29], induce site-specific DNA double strand breaks (DSBs) at chosen sites. These DSBs activate one of two major DNA repair mechanisms, NHEJ or homology directed repair (HDR), which can be employed to disrupt genes or to target the integration of exogenous donor DNA sequences to a specific site in the genome, respectively [30].

The goal of this study was to establish an *in vitro* disease model for T-cell deficiencies and to employ this model to evaluate a designer nuclease-based genome editing strategy. To this end, we generated iPSCs from adult ear fibroblasts of NOD.SCID mice, a model for RS-SCID [31], and established a protocol to recapitulate T-lymphopoiesis from iPSCs *in vitro*. We used ZFNs to edit DNA-PK deficient fibroblasts and iPSCs and demonstrated that designer nuclease mediated gene correction led to rescue of DNA-PK dependent signaling, normal radiosensitivity, restoration of T-cell maturation, and polyclonal TCR recombination. We hence provide proof that the combination of two promising technology platforms, iPSCs and designer nucleases, with a protocol to generate T-cells *in vitro* represents a powerful paradigm for SCID disease modeling and the evaluation of therapeutic gene editing strategies.

Results

Restoring DNA-PK activity in SCID fibroblasts by targeted genome editing

In the murine disease model RS-SCID is caused by a T-to-A transversion mutation in exon 85 of the *prkdc* locus. The introduced premature stop codon (Y4046*) leads to an 83 aa long C-terminal truncation of the encoded DNA-PKcs protein, leading to decreased protein stability and low kinase activity [31]. ZFNs targeted to intron 84 of *prkdc* were generated using the OPEN platform [32] and their activity verified by *in vitro* cleavage assays and plasmid-based recombination assays (S1 Fig). To restore function of DNA-PK, we generated a donor DNA encompassing the wild-type cDNA sequence of *prkdc* exons 85 and 86, preceded by a splice acceptor

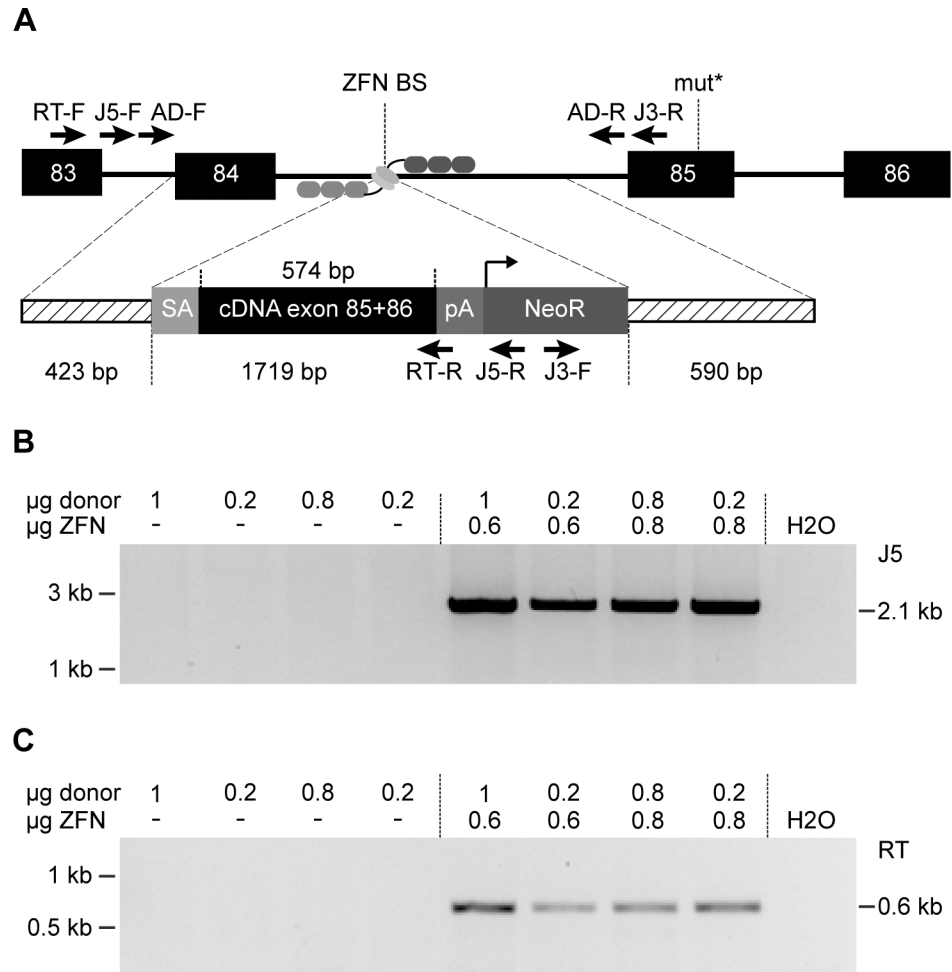


Fig 1. Targeted genome editing in RS-SCID fibroblasts. (A) Schematic of genome editing strategy. Homology-directed repair (HDR) between the *prkdc* locus and the donor DNA is promoted by ZFN cleavage in intron 84 (BS, binding site). The HDR donor consists of flanking homology arms (dashed lines), splice acceptor (SA), cDNA encoding *prkdc* exons 85 and 86, polyadenylation signal (pA), neomycin resistance cassette (*NeoR*). The SCID underlying mutation in exon 85 (mut*), and primer binding sites for PCR analysis (5'-junction J5-F/J5-R; 3'-junction J3-F/J3-R; allelic discrimination AD-F/AD-R; mRNA expression RT-F/RT-R) are indicated. (B) Genome editing. After transfection of SCID fibroblasts with various ratios of donor DNA to ZFN expression plasmids, successful gene targeting in polyclonal samples was detected by an inside-out PCR amplification of the genome-donor 5'-junction (J5-F/J5-R). (C) Expression of corrected *prkdc* mRNA. After transfection of SCID fibroblasts, successful splicing from exon 83 to cDNA was detected with an inside-out RT-PCR strategy using primers RT-F/RT-R.

doi:10.1371/journal.pgen.1005239.g001

site and followed by a poly(A) signal (Fig 1A). Targeting an intron allowed us to co-introduce a neomycin selection marker cassette to enrich for cells that underwent correct gene targeting.

To validate our targeting strategy, fibroblasts from a 12-week old male NOD.SCID mouse, in which the SCID mutation in *prkdc* was confirmed by sequencing, were isolated. Upon culturing *in vitro* these cells transformed spontaneously, probably due to their intrinsic DNA repair deficiency. The fibroblasts were transfected with various ratios of donor DNA to ZFN expression plasmids before G418 selection was applied. An inside-out PCR strategy was used to verify correct gene targeting in polyclonal cell populations (Fig 1B). All samples transfected with ZFN expression plasmids and donor revealed successful gene targeting. Splicing of exon 84 to the integrated cDNA was verified by inside-out reverse transcription (RT)-PCR (Fig 1C).

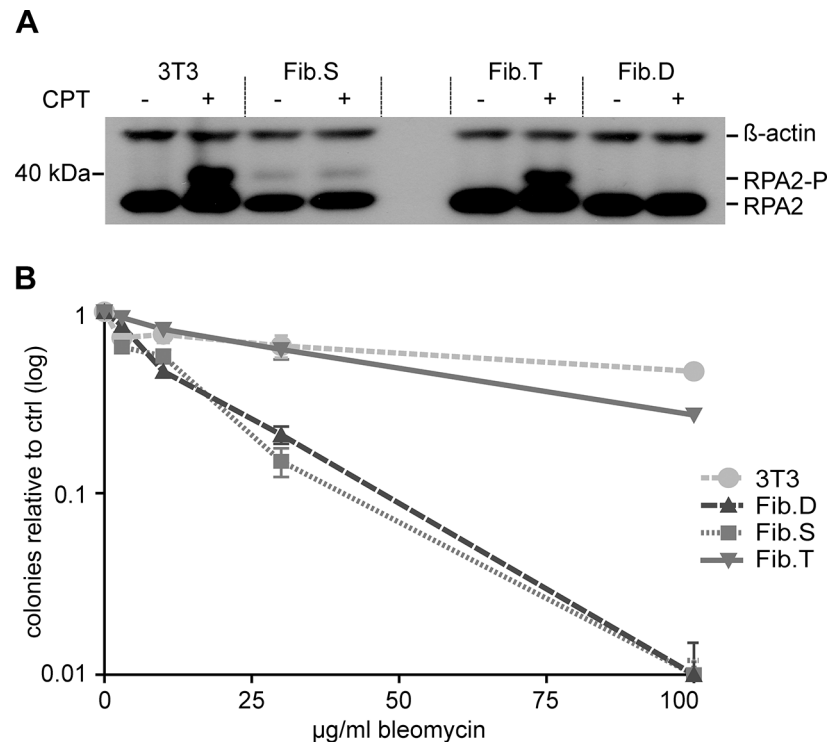


Fig 2. Functional correction of RS-SCID fibroblasts. (A) DNA-PK dependent phosphorylation of RPA2. Treatment of fibroblasts with camptothecin (CPT) induces DNA-PK dependent phosphorylation of RPA2, which was detected by Western blot analysis using an RPA2 specific antibody. Detection of β-actin served as a loading control. Positions of RPA2 and its phosphorylated form, RPA2-P, are indicated on the right. (B) Rescue of radiosensitivity. Fibroblasts were cultured with increasing amounts of the radiomimetic drug bleomycin. Cellular sensitivity to the drug was quantified by counting number of surviving colonies relative to untreated samples. Data are represented as mean ± SD (N = 3). 3T3, NIH-3T3 fibroblasts; Fib.S, SCID fibroblasts; Fib.T, gene targeted SCID fibroblasts; Fib.D, fibroblasts treated with randomly integrated donor.

doi:10.1371/journal.pgen.1005239.g002

To determine the efficiency of the gene targeting approach, cell clones were generated by single cell dilution. Six out of 20 analyzed clones showed correct targeting.

To confirm that re-routed splicing of exon 84 to the artificial exon 85/86 restored DNA-PK activity, cells were treated with camptothecin (CPT), a compound known to induce DSBs during DNA replication by blocking topoisomerase I. Under these experimental conditions, RPA2 is exclusively phosphorylated by DNA-PK at the stalled replication forks [33]. Upon CPT treatment of SCID fibroblasts (Fib.S), a gene edited fibroblast clone (Fib.T) and a donor-containing clone (Fib.D), phosphorylation of RPA2 was detected in Fib.T cells, but not in Fib.S and Fib.D cells (Fig 2A). The fibroblast cell line NIH-3T3 served as a positive control.

Fibroblasts of RS-SCID mice are sensitive to gamma-irradiation or the radiomimetic drug bleomycin [34]. To verify that successful gene targeting could abrogate radiosensitivity, colony survival assays with bleomycin were conducted. We found that the corrected cell line Fib.T displayed similar resistance to the drug as NIH-3T3 cells, while both Fib.D and Fib.S cells were highly sensitive to bleomycin (Fig 2B). In conclusion, successful ZFN-mediated genome editing restored activity of DNA-PK, which was able to phosphorylate downstream target proteins and to rescue the radiosensitive phenotype of RS-SCID cells.

Genetic correction of SCID iPSCs

While fibroblasts served as an important model to evaluate DNA-PK dependent signaling, the full therapeutic potential of genome editing at the *prkdc* locus can only be assessed in lymphoid cells. iPSCs have the capacity for unlimited self-renewal, allowing long-term *in vitro* culture and generation of single-cell derived subclones. As iPSCs can be differentiated into hematopoietic cells, including T lymphocytes, they are an ideal platform for disease modeling and the evaluation of gene therapeutic approaches. We generated iPSCs from fibroblasts isolated from a 6-week-old NOD.SCID mouse by transduction with a polycistronic lentiviral vector expressing the reprogramming factors Oct4, Klf4, Sox2 and c-Myc [35]. Since the DNA repair-deficient phenotype interferes with efficient reprogramming [36], we conducted the experiment under hypoxic conditions and added ascorbic acid to reduce damage by reactive oxygen species (ROS) [37]. In addition, small molecule inhibitors for MAP kinase (MEK), glycogen synthase kinase 3 (GSK3) and TGF-beta were used, which have been reported to permit derivation of iPSCs of NOD-derived mouse strains and enhance the reprogramming progress [38,39]. All analyzed iPSC clones expressed pluripotent stem cell markers (S2 Fig), and RT-PCR demonstrated expression of the embryonic stem cell-specific genes in a NOD.SCID iPSC clone (iPS.S6; Fig 3A). In addition, cells from ectodermal (neural rosette-like structures), endodermal (gut-like structures) and mesodermal (smooth muscle patches) origin were detected in teratoma derived from clone iPS.S6 (Fig 3B). Genome integrity was assessed before and after ZFN mediated genome engineering by spectral karyotyping (Figs 3C and S2). The NOD.SCID iPSC clone iPS.S6 displayed no gross genetic abnormalities and was used for subsequent gene targeting experiments. In summary, we showed that DNA-repair deficient NOD.SCID fibroblasts could be reprogrammed into iPSCs that display pluripotent behavior and characteristics similar to murine embryonic stem cells.

For targeted genome editing, cells of iPSC clone iPS.S6 were nucleofected with donor and ZFN expression plasmids. Following selection and clonal expansion, inside-out PCR amplification was applied on genomic DNA to detect correct targeting. Of note, 41 out of 46 analyzed clones (89%) showed correct integration of the artificial exon 85/86. Extended PCR analysis of five targeted iPSC clones verified correct 5' - and 3' -junctions between genomic and donor DNA, respectively. An allelic discrimination PCR confirmed mono-allelic targeting in all cases (Fig 4A). Furthermore, expression of the DNA-PKcs encoding mRNA and re-routed splicing to artificial exon 85/86 was validated by inside-out RT-PCR (Fig 4B). All targeted iPSC clones were positive for expression of pluripotency markers (Fig 3A), formed all three germ layers in teratoma assays (Figs 3B and S2), had an intact karyotype (Figs 3C and S2), and did not show any signs of NHEJ-mediated mutagenesis at the top 15 predicted off-target sites in the mouse genome (S1 Table, S1 Text).

The polycistronic lentiviral vector used for generation of iPSCs contained Flp recognition target (FRT) sites in the U3 region of the long-terminal repeats, which allowed us to excise the reprogramming cassette using retroviral-mediated transfer of Flp recombinase [40]. Southern blot analysis confirmed successful removal of the lentiviral vector genome (S3 Fig) and targeted integration of the artificial exon 85/86 into intron 84 of the *prkdc* locus (S3 Fig).

Differentiation of iPSCs to TCR-positive T lymphocytes

Since DNA-PK is essential for V(D)J recombination, the RS-SCID immunophenotype is characterized by a lack of T and B-lymphocytes [41]. The stromal cell line OP9-DL1 leads to activation of the DL1-mediated Notch signaling in co-cultured cells, which in turn is a prerequisite to induce the T-lymphoid program in multipotent hematopoietic progenitors [24]. Initial experiments showed that OP9-DL1 co-cultivation of C57BL/6-derived lineage negative bone

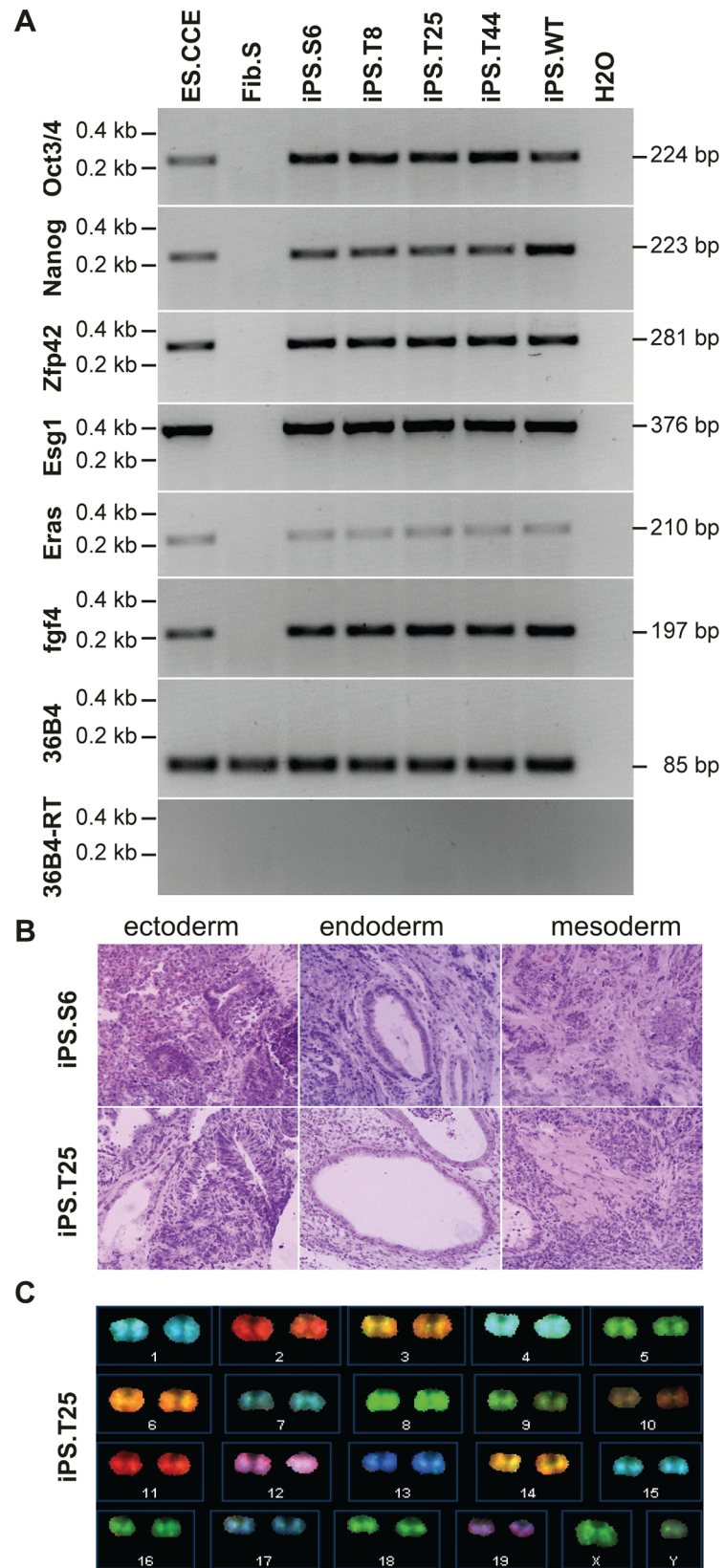


Fig 3. Evaluation of pluripotency of generated iPSCs. (A) Pluripotent stem cell marker gene expression. Oct3/4, Nanog, Zfp42, Esg1, Eras, and fgf4 mRNA expression was determined by qualitative RT-PCR (see S2 Table). Housekeeping gene 36B4 (+/- reverse transcriptase) were included as controls. ES.CCE, murine embryonic stem cell line; Fib.S, SCID fibroblasts; iPS.S6, SCID iPSC clone; iPS.T8, iPS.T25, iPS.T44, gene targeted SCID iPSC clones; iPS.WT, wild-type iPSC clone. (B) *In vivo* differentiation analysis. Teratoma formation was induced by subcutaneous injection of iPSCs into mice. **Hematoxylin/eosin**-stained sections of teratoma-derived from clones iPS.S6 and iPS.T25 are shown. (C) Karyotype analysis. Spectral karyotyping (SKY) was performed to detect microscopic genomic abnormalities, translocations and aneuploidies in untreated or genetically corrected SCID iPSC clones. SKY analysis of clone iPSC.T25 is shown (see also S2 Fig).

doi:10.1371/journal.pgen.1005239.g003

marrow cells enabled the differentiation of these multipotent stem cells through all (CD4⁻/CD8⁻) double-negative (DN) thymocyte stages, as determined by CD25 and CD44 surface expression. Further culturing of these T-cell precursors on OP9-DL1 led to the generation of CD4⁺/CD8⁺ double-positive (DP) T lymphocytes, which expressed the beta chain of the T-cell receptor (TCR β), indicating that these cells have successfully undergone V(D)J recombination and beta-selection *in vitro* (Fig 5).

Since V(D)J recombination is initiated at the DN2 (CD44⁺/CD25⁺) stage and beta-selection occurs at the DN3 (CD44⁻/CD25⁺) stage, we hypothesized that corrected RS-SCID iPSC-derived hematopoietic progenitor cells (HPCs) should be able to differentiate to CD4⁺/CD8⁺ double-positive T lymphocytes, while T-cells derived from uncorrected SCID-derived iPSCs would stop at the DN2 thymocyte stage due to their defect in V(D)J recombination (Fig 5A).

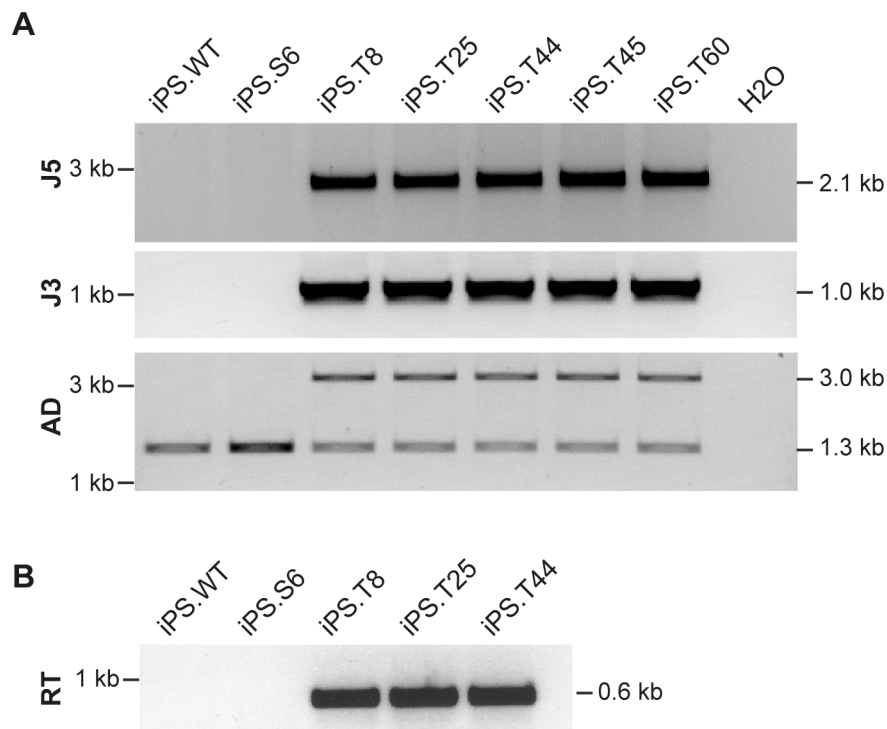


Fig 4. Targeted genome editing in SCID-derived iPSCs. (A) Verification of gene targeting. Inside-out PCR strategies (see Fig 1A) were used to verify correct 5' (J5) and 3' (J3) junctions of the integrated donor. Allelic discrimination (AD) PCR was used to assess mono- vs. bi-allelic integration. Targeted allele runs at 2.99 kb. Sizes of all expected PCR amplicons are indicated on the right. iPS.WT, wild-type iPSC; iPS.S6, SCID iPSC clone; iPS.T8, iPS.T25, iPS.T44, iPS.T45 and iPS.T60, targeted SCID iPSC clones. (B) Expression of corrected *prkdc* mRNA. Successful splicing from exon 83 to cDNA encompassing exons 84/85 was detected by an inside-out RT-PCR strategy using primers RT-F/RT-R.

doi:10.1371/journal.pgen.1005239.g004

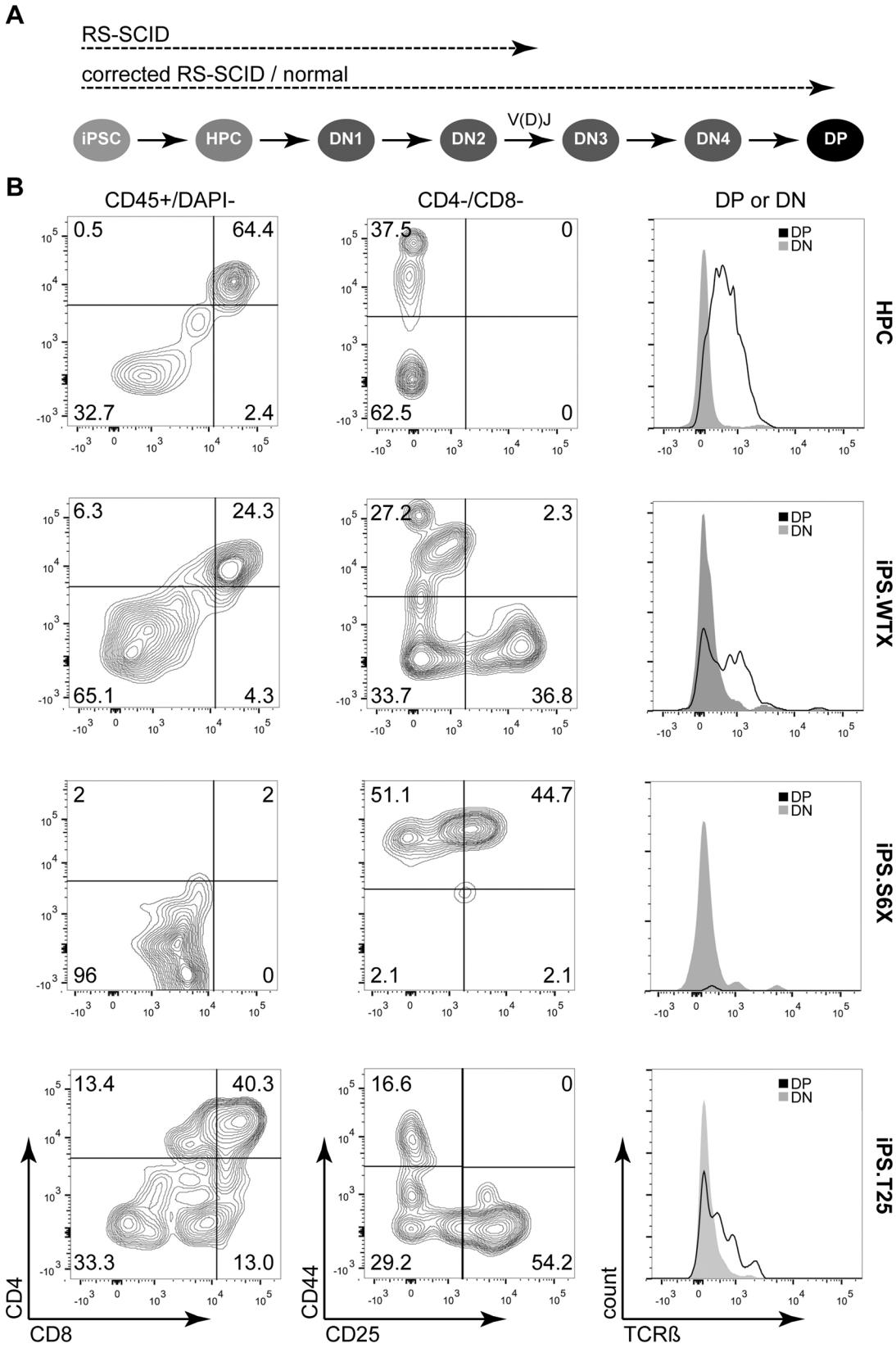


Fig 5. *In vitro* differentiation of iPSCs to proT-cells and T-cells. (A) Schematic of *in vitro* T-cell differentiation from iPSCs. Differentiation of iPSCs starts with formation of embryoid bodies that are dissociated to give rise to hematopoietic stem and progenitor cells (HPC). DL-1 mediated Notch signaling coaxes HPC development towards early proT-cells (DN2), which undergo DNA-PK dependent V(D)J recombination. After passing through DN3 and DN4 stages, preT-cells mature into double-positive (DP) T-cells that express the beta chain of the T-cell receptor (TCR β). Dashed lines indicate to what stage iPSC clones are expected to differentiate. (B) Assessment of T-cell differentiation. *In vitro* T-cell differentiation was analyzed by flow cytometry after two weeks of co-cultivation on OP9-DL1. Gating (indicated on top of each column) was applied in the following order: FSC/SSC and CD45⁺/DAPI⁻ to assess CD4/CD8 expression; CD8⁻/CD4⁻ to gate for DN1-DN4 stage cells; CD8⁻/CD4⁻ (DN) or CD8⁺/CD4⁺ (DP) to assess TCR β expression. Numbers indicate percentage of cells in each quadrant. HPC, lineage-negative bone marrow cells; iPS.WTX, wild-type iPSC; iPS.S6X, SCID iPSC clone; iPS.T25, gene targeted SCID iPSC clone.

doi:10.1371/journal.pgen.1005239.g005

To this end, we established an embryoid body (EB)-based differentiation protocol for the generation of HPCs from iPSCs. Differentiated and dissociated EBs from all iPSC clones contained cells carrying the early hematopoietic surface markers CD41 and cKit (S4 Fig). Co-cultivation of these cells on OP9-DL1 stroma cells induced differentiation towards T-lymphocytes. After two weeks, thymocyte maturation of iPSC-derived HPCs was measured by flow cytometry, revealing the presence of CD44⁺/CD25⁻ (DN1), CD44⁺/CD25⁺ (DN2), CD44⁻/CD25⁺ (DN3), CD44⁻/CD25⁻ (DN4), and CD4⁺/CD8⁺ (DP) cells from wild-type iPSCs (iPS.WTX; Fig 5). As hypothesized, T-cell differentiation of NOD.SCID iPSCs (iPS.S6X) was blocked in early DN1 and DN2 thymocyte stages and these T-cell precursors showed neither expression of CD4/CD8 nor TCR β . In contrast, differentiation from genetically corrected iPSC clones (iPS.T25X) reached DN3 and DN4 stages as well as the CD4⁺/CD8⁺ DP T-cell stage, with a fraction of cells expressing TCR β (Fig 5B). Although the same experimental conditions were applied, the absolute numbers of generated T-cells varied in between different experiments.

To confirm T-cell receptor recombination on the genome level, V(D)J recombination was verified by spectratyping. Control T-cells isolated from the thymus and *in vitro* generated T-cells from bone marrow lineage negative cells showed a polyclonal T-cell repertoire at V β chains 1, 6, 8.1, 8.3, 10, 12, 14 and 20 (Figs 6 and S5). While V(D)J recombination was undetectable in T-cell precursors derived from SCID iPSCs, T lymphocytes derived from WT or gene targeted iPSCs underwent V(D)J recombination and revealed a polyclonal T-cell repertoire.

In summary, we developed a protocol, which allowed us to model T-cell differentiation *in vitro*. We showed that iPSCs can be differentiated into hematopoietic progenitors and further to various stages of thymocyte development. While wild-type and corrected NOD.SCID iPSCs could be matured into CD45⁺ CD4⁺/CD8⁺ DP T-cells that express TCR β , differentiation of DNA-PK-deficient cells stopped at the DN2 thymocyte stage. These results provide a proof of concept that iPSC-based *in vitro* disease modeling is able to reflect *in vivo* thymocyte maturation and that such modeling can be used for both to investigate T-cell maturation defects and to validate gene therapy strategies.

Discussion

SCID is a group of monogenetic disorders of the immune system characterized by the absence of T-cells, sometimes in combination with a lack of functional B-lymphocytes and/or natural killer cells. RS-SCID is a special form of SCID disorders and serves as a paradigm for radiosensitivity and immunodeficiency. On top of the absence of T- and B-lymphocytes, the pathophysiology of RS-SCID is characterized by a strong sensitivity of all somatic cells to radiation and DNA damaging agents due to a defective DNA repair pathway. The underlying mutations are found in genes coding for NHEJ factors, including LIG4 [42], Artemis [43], XLF [44] and DNA-PKcs [9].

Disease modeling based on patient-derived iPSCs is particularly valuable when studying rare disorders, like RS-SCID, for which patient cells are not easily accessible, have a limited

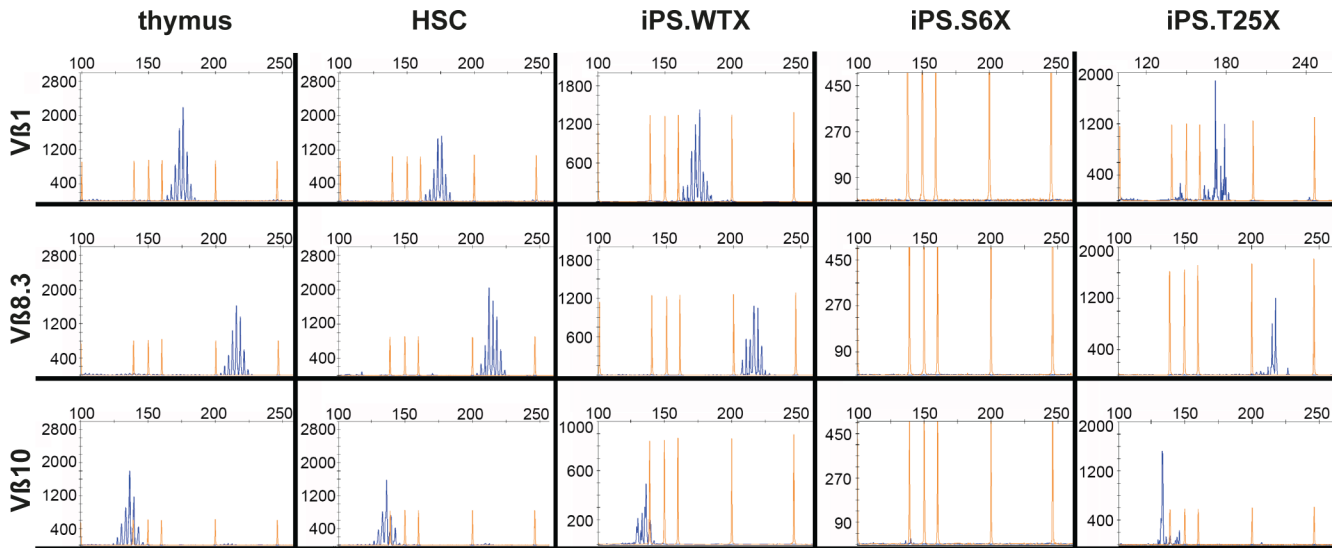


Fig 6. Polyclonal T-cell receptor recombination. *In vitro* generated T-cells were analyzed by spectratyping, i.e. quantitative RT-PCR expression analysis of the variable beta chains. Exemplarily shown are results for Vβ1, Vβ8.3 and Vβ10 (see also S5 Fig). X-axis depicts detected PCR fragment size in bp, Y-axis depicts counts of obtained PCR fragments. Thymus, T-cells isolated from thymus as a positive control; HSC, *in vitro* generated T-cells from lineage-negative bone marrow cells; iPS.WTX, wild-type iPSCs; iPS.S6X, SCID iPSC clone; iPS.T25X, gene targeted SCID iPSC clone.

doi:10.1371/journal.pgen.1005239.g006

lifespan, or do not develop due to a differentiation block. Designer nuclease-based gene editing in iPSCs makes this instrument even more attractive because it enables scientists to correlate genotype to phenotype in an isogenic background, either by creating disease models through the insertion of disease specific mutations in normal cells [45] or by correcting the underlying genetic mutation back to wild-type in patient-derived iPSCs [16,46]. Particularly in combination with genetic engineering, iPSCs are preferred over fibroblasts because of their unlimited proliferative potential and their ability of clonal expansion.

Hematopoietic differentiation protocols offer the possibility to investigate maturation of various blood lineages *in vitro*, e. g. to study the impact of genomic mutations on protein function in mature blood cells or where specific mutations lead to a block in lymphopoiesis, myelopoiesis, or erythropoiesis [17,18,46]. While designer nuclease-based gene editing in iPSCs has been established in several labs, differentiation of genetically modified iPSCs to mature immune cells has remained challenging. Differentiation of iPSCs derived from a patient suffering from X-linked chronic granulomatous disease (X-CGD) to granulocytes was the first example to show functional correction of a genetic defect by targeted integration of a gp91^{phox} expression cassette into the putative safe harbor site AAVSI [15]. Myeloid differentiation from patient-derived iPSCs for disease modeling and/or drug development has also been established e.g. for severe congenital neutropenia [47] and pulmonary alveolar proteinosis [20].

Differentiation of iPSCs to lymphocytes, on the other hand, has been reported only from a few labs [18,19]. In the present study, we describe an improved *in vitro* differentiation procedure for iPSCs to T-cells that is based on previously published protocols [18,48,49], and, to our knowledge, use this protocol for the first time to model the functional defects of an immunodeficiency *in vitro* and to investigate the effect of genetic engineering of disease iPSCs on T-cell maturation. Because the generated hematopoietic progenitor cells supported the maturation through all early stages of thymocyte differentiation, including V(D)J recombination and beta-selection, we were able to reproduce the stage-specific block induced by the point mutation in the *prkdc* locus *in vitro*. This setup can also be used to screen for genotype-phenotype

correlations or to characterize the consequence of newly identified genetic mutations on T-lymphopoiesis and/or T-lymphocyte function in more detail. For instance, as compared to *in vivo* models, individual effects of the microenvironment, cytokines and/or small molecules affecting T-cell maturation and expansion, like IL-7 or IL-2, can be analyzed by simple addition to the culture medium. Moreover, existing stroma-free models can be further developed [50] to identify factors downstream of Delta-like Notch ligands that promote T-cell development. Finally, the efficiency of T-cell related gene therapy approaches can be assessed *in vitro*, without the need of hematopoietic stem cells of the patients.

In our study we applied ZFNs for genetic modification of RS-SCID iPSCs. The generation of highly specific ZFNs can be rather challenging and several studies have described off-target cleavage activity of ZFNs [51,52]. While the specificity of ZFNs can be improved, e.g. by optimizing the DNA binding properties of the zinc-finger arrays [32], selecting appropriate linker domains [53,54] and employing obligate heterodimeric *FokI* nuclease domains [55,56], alternative designer nucleases, such as TALENs [28] and CRISPR/Cas9 based nucleases [29], are easier to engineer.

Our system provides a basis for further development of iPSC-derived cell products with the potential for various clinical applications. However, although we have tried to transplant iPSC-derived hematopoietic stem/precursor cells into NOD.SCID mice, we did not observe any engraftment of these cells. This is in line with published data showing that transplantation worked only with iPSC-derived hematopoietic stem/precursor cells that were produced *in vivo* [22,23]. Further studies will be needed to establish optimal culture conditions to generate transplantable stem cells *in vitro*. Hence, combining *in vitro* protocols with physiologic *in vivo* differentiation seems more promising. For example, transplantation of iPSC-derived early thymocyte progenitor populations could allow for thymic reconstitution and maturation to create polyclonal T-cell effector populations [50]. Infusions of *in vitro* derived autologous T-cells could be used to stabilize patients suffering from primary immunodeficiencies, like SCID or hemophagocytic lymphohistiocytosis, or after conventional hematopoietic stem cell transplantation to close the gap until graft-derived lymphocytes arise. Moreover, given the clinical success of autologous T-cells expressing tumor specific chimeric antigen receptors (CARs) [57], iPSC-derived autologous CAR-T-cells represent an interesting alternative to current protocols, as recently shown [19]. Finally, autologous, CCR5 knockout iPSC lines could present a source to provide HIV patients with HIV-resistant T-cells to reconstitute the adaptive immune system [58]. However, before iPSC-based cell therapies can enter clinical practice, safety concerns, especially with regard to the generation of iPSC-derived teratoma, have to be addressed and full functionality of iPSC-derived cells proven.

In conclusion, our study describes an iPSC-based disease model for RS-SCID. Our *in vitro* protocol allowed us to differentiate iPSCs to T-cells and to analyze the influence of NHEJ deficiency on V(D)J recombination. Moreover, it emphasizes the significance of designer nucleases as a tool in generating isogenic disease models and their future role in producing iPSC-based, patient-specific, genetically corrected autologous transplants for various applications in the clinic.

Materials and Methods

Cells and cell culture

NIH.3T3 and HEK293T cells were cultured in DMEM (Biochrom) supplemented with 10% FCS (PAA), penicillin/streptomycin (P/S; PAA), L-glutamine (Biochrom) and sodium pyruvate (PAA). OP9 and OP9-DL1 cells (obtained from Juan Carlos Zúñiga-Pflücker) were expanded in OP9 medium [α -MEM (Gibco), 20% OP9-tested FCS (PAA), P/S and

L-glutamine]. Primary mouse ear fibroblasts were cultured in MEF medium [DMEM low glucose (PAA) with 15% FCS, L-glutamine, nonessential amino acids (NEAA; Gibco), P/S, 100 μ M of β -mercaptoethanol (Sigma-Aldrich), sodium pyruvate and 50 μ g/ μ l phospho-ascorbic acid (P-VitC, Sigma-Aldrich)]. ES.CCE cells were cultivated in ES medium [Knockout-DMEM (Gibco) with 15% ES-tested FCS (PAA), P/S, L-glutamine, NEAA, 150 mM monothio-glycerol (MTG, Sigma-Aldrich) and ESGRO mouse LiF (Millipore)]. iPSCs were cultivated in iPSC medium [Knockout-DMEM supplemented with 15% ES-tested FCS, NEAA, P/S, L-Glutamine, 100 μ M of β -mercaptoethanol and ESGRO mouse LiF, 50 μ g/ μ l of P-VitC, 4 μ M of SB431542, 1 μ M of PD0325901 and 3 μ M of CHIR99021 (all Axon Medchem, together termed 3i) and passaged with Accutase (Gibco). ES.CCE cells and iPSCs were cultivated either on irradiated C3H or CF-1 MEF feeders on gelatin-coated plates or feeder-free in vented flasks (Sarstedt). Lineage negative cells (HSC) were isolated by flushing the tibiae and femurs of C57BL/6N mice (Charles River) and purified by magnetic cell sorting (MACS) with the Lineage Cell Depletion Kit (MACS Miltenyi) according to the manufacturer's protocol. Cells were stained with Trypan Blue (Sigma-Aldrich) and counted at 100x microscope magnification prior to *in vitro* T-cell differentiation. Cell clones were generated either by limiting dilution (fibroblasts) or colony picking (iPSCs). All but HEK293T cells were cultivated under hypoxic conditions (7% CO₂ / 5% O₂).

Plasmids

Prkdc-specific zinc-finger arrays (S1 Fig) were generated with the OPEN protocol [32]. To generate ZFNs, the zinc-finger arrays were codon-optimized (GeneArt) and cloned into pRK5 vectors, with and without NLS [59], containing the cleavage domains of wild-type *FokI* or the obligate heterodimeric *FokI* variant KV/EA [55] and the LRGS linker [54]. The target plasmid pCMV.LacZsPK Δ GFP was generated by replacing the "31" target site of pCMV.LacZs31 Δ GFP [59] by the ZFN target site aGTTTGCGCCtaactGAAGGTGACa (capital letters indicate target site for ZFN). The donor plasmid pJet.SAE8586Neo (Fig 1A) consists of (i) a splice acceptor (SA) [60]; (ii) a cDNA consisting of *prkdc* exons 85 and 86, which was PCR amplified from pMEPK7 (kindly provided by Masumi Abe) with primers PRK-F/PRK-R (S2 Table); (iii) an SV40 polyadenylation signal (pA); (iv) a *NeoR* cassette comprise the aminoglycoside phosphotransferase coding sequence flanked by the HSV thymidine kinase promoter and an SV40 pA (kindly provided by Stefan Weger); (v) left and right homology arms, which were PCR amplified from Fib.S gDNA.

Characterization of ZFN

For expression analysis, ZFNs were expressed in HEK293T for immunoblotting as previously described [59]. The *in vitro* cleavage assay was basically performed as defined before [61]. Briefly, a target DNA was amplified by PCR from Fib.S gDNA using primers IV-F/IV-R (S2 Table). ZFNs were *in vitro* transcribed/translated with the TNT SP6 Coupled Reticulocytes Ly-sate System (Promega), 150 ng of target DNA was mixed with the reticulocyte lysates, incubated for 1.5 h at 37°C, and analyzed on a 1.5% agarose gel. The plasmid-based gene targeting assay was conducted as described before [59]. Flow cytometry to determine the percentage of EGFP and REX positive cells was performed on FACSCalibur with CellQuestPro software (BD Biosciences).

Gene targeting in RS-SCID cells

For targeted integration into Fib.S fibroblasts, 1x10⁵ cells were transfected 24 h after seeding with Lipofectamine 2000 (Life Technologies). 1.6 μ g of endotoxin-free DNA was mixed with

4.8 μ l of transfection reagent in 200 μ l OptiMEM (Gibco). The ZFN expression plasmids were co-transfected with the donor pJet.SAE8586Neo at different ratios and filled up with pUC118 to 1.6 μ g. Selection with 500 μ g/ml of G418 (Sigma-Aldrich) was applied 5 days after transfection for 7 days. iPSCs were grown feeder-free before and after transfection. 3×10^6 cells were nucleofected with 10 μ g of pJET.SAE8586Neo and 5 μ g of each ZFN expression plasmid using the Mouse ES Cell Nucleofector Kit (LONZA) and Nucleofector II with program A-030. After 5 days of recovery, G418 selection was applied for 7 days at a concentration of 400 μ g/ml. After 1 week, iPSC clones were isolated and cultivated on feeders.

Genotyping by PCR or Southern blotting

Genomic DNA was extracted with the QIAamp DNA Blood Mini Kit (QIAGEN). G418 selected fibroblast and iPSC clones were analyzed for legitimate targeted integration by inside-out PCR using Phire Hot Start II DNA polymerase kit (Thermo Scientific). RNA was isolated with TRIzol (Life Technologies), and all RT-PCR reactions performed with the QuantiTect Reverse Transcription Kit (QIAGEN). All used primers are listed in [S2 Table](#). For Southern blot analysis [62], genomic DNA was digested with *EcoRV* or *BamHI*, separated on a 0.8% agarose gel and transferred to Biotodyne B nylon membrane (PALL Life Sciences). DNA was hybridized with a 32 P-labeled fragment of PRE (for detection of the reprogramming vector) or NeoR (for detection of donor copies) using the DecaLabel DNA Labeling Kit (Fermentas). Labeled *HindIII* digested Lambda DNA was used as a marker.

Functional tests to assay DNA-PK activity

To measure DNA-PK dependent RPA2 phosphorylation, 8×10^5 fibroblasts were treated with 1 μ M of camptothecin (Sigma-Aldrich) for 1 h. Cells were harvested in RIPA buffer supplemented with Complete Protease Inhibitor and PhosSTOP phosphatase inhibitor cocktails (both Roche). Western blot was basically performed as described before [63,64]. RPA2 and β -actin were detected with rat anti-RPA32 (1:1000, 4E4, Cell Signaling) and rabbit anti- β -actin (1:1000, Cell Signaling), respectively, and visualized with HRP-conjugated anti-rat and anti-rabbit antibodies (1:20,000, Dianova) and West Pico Chemiluminescence substrate (Thermo Scientific). For the colony survival assay, 1×10^5 fibroblasts were treated 1 day after seeding with the indicated amounts of bleomycin (Sigma-Aldrich) for 2 h. Cells were washed with PBS, trypsinized and 5,000 cells seeded into a 10-cm plate ($N = 3$). After 4 days the plates were stained with 0.5% (w/MeOH) crystal violet (Sigma-Aldrich) and colonies counted.

Generation, excision and characterization of iPSC

Murine adult fibroblasts were extracted from ears of 6-week old NOD/ShiLtJ and NOD.CB17-Prkdc scid/J male mice as described before [62]. Fibroblast from 12-week old NOD.CB17-Prkdc scid/J mouse gave rise to spontaneously transformed Fib.S. The “4-in-1” reprogramming vector pRRL.PPT.SF.mOKSMco.idTom.PRE, co-expressing the transcription factors Oct4, Klf4, Sox2 and c-Myc with the fluorescent marker tdTomato, has been previously described [35]. To generate versions that allow for Flp recombinase-mediated excision (pRRL.PPT.SF.mOKSMco.idTom.PRE.FRT), FRT sites were introduced into the promoter-deprived U3 region. Virus production has been described elsewhere [65]. The reprogramming was conducted as described before [35]. Briefly, NOD.CB17-Prkdc scid/J or NOD/ShiLtJ-derived fibroblasts were seeded in MEF medium on gelatin-coated 6-well-plates at 8×10^4 /well for transduction. After 2 days, cells were transduced with an MOI of 5 and incubated for 8 h, following 2 times washing with PBS. MEF medium with 2 mM VPA (Sigma Aldrich) was added. After 4 days medium was changed to iPS medium with VPA, and after 7 days 3i was added. After 14

days, emerging iPSC colonies were isolated and expanded for characterization. A total of 12 iPSC clones derived from NOD.CB17-Prkdc scid/J (iPS.S) were initially characterized by assessing expression of SSEA-1 by flow cytometry and staining of alkaline phosphatase (Millipore) followed by documentation with the Olympus IX71 system. Determination of the vector copy number (VCN), teratoma formation, Flp recombinase-mediated excision, fluorescence *in situ* hybridization (FISH) and pluripotency factors RT-PCR analysis have been described previously [35,62,66]. Clone iPS.S6 was used for gene targeting and three out of 41 corrected clones (iPS.T8, iPS.T25, iPS.T44) were characterized in detail. The parental uncorrected clone iPS.S6 was included as a negative control, a wild-type NOD/ShiLtJ derived clone (iPS.WT) as a positive control.

In vitro T-cell differentiation

The protocol was adapted from previously published work [48,49]. For embryoid body (EB) formation, iPSCs were split with Collagenase IV (Gibco) and 5×10^4 cells were cultured in suspension plates in 2 ml of EB medium [IMDM (Biochrom AG) with 15% ES cult FCS (Stem Cell Technologies), 5% PFHM II (Gibco), P/S, L-Glutamine, 50 μ g/ml P-VitC, 150 mM MTG, 200 μ g/ml human transferrin (Sigma-Aldrich)] in a normoxic incubator on a shaker at 60 rpm. At day 2.5, 0.5 ml of EB medium plus cytokines rhBMP-4, activinA, rhVEGF165 and rhFGF-2 at 5 ng/ml final concentration each (all R&D Systems) was added. At day 8, EBs were harvested, washed with PBS and collected in Trypsin-EDTA, diluted 1:15 in Collagenase IV. After 30 min, 2.5 ml of cell dissociation buffer (Gibco) was added and cells transferred through a 70- μ m mesh. Hematopoietic progenitor cells (HPCs) were washed with PBS and analyzed for CD41/cKit expression by flow cytometry prior to hematopoietic expansion. To this end, 10^6 EB-derived HPCs were cultivated for 3 days under hypoxic conditions in STFV medium [IMDM, 10% OP9-tested FCS, P/S, L-glutamine, 10 ng/ml mSCF, 20 ng/ml mTPO, 100 ng/ml rhFlt3-L (all Peprotech), and 40 ng/ml rhVEGF165 (R&D Systems) (final concentration each)]. At day 3, cells were harvested through a 100- μ m mesh and washed with PBS prior to *in vitro* T-cell differentiation. To this end, up to 3×10^5 expanded HPCs or $0.5\text{--}1 \times 10^5$ HSCs were added in T-cell differentiation medium [OP9 medium, supplemented with 1 ng/ml mIL-7 (Peprotech) and 5 ng/ml rhFlt3-L]. After 3 days, 2 ml medium was added and cultivation continued for up to 4 weeks. Every 7 days cells were harvested through a 100- μ m mesh, washed with PBS, transferred to a new OP9-DL1 cell layer, and analyzed for T-cell differentiation by flow cytometry.

Analysis of T-cell phenotype and genotype

For flow cytometric analysis, cells were resuspended in FACS buffer [PBS supplemented with 2% FCS, 1 mM EDTA and 0.1% sodium azide (both Sigma-Aldrich)]. To stain for pluripotency marker SSEA-1, iPSCs were rinsed with PBS and stained with biotinylated anti-SSEA-1 antibody (eBioscience) diluted in FACS buffer for 20 min at 4°C. After rinsing the secondary staining was performed with a streptavidin-APC antibody (eBioscience). Hematopoietic cells were pretreated with Mouse BD Fc block (BD Biosciences) before antibody staining. Antibody staining was performed for 20 min at 4°C. EB-derived HPCs were stained with CD41-PE, cKit-APC, or respective isotype controls (all eBioscience). iPSC-derived T-cells were stained with CD44-PE and CD25-APC, or CD4-PE and CD8-APC. Viability staining with 7-AAD was performed for 2 min during the last rinsing, before samples were measured on a FACSCalibur. Alternatively, iPSC-derived T-cells were stained with CD45-APC-Cy7, CD4-PerCPR-Cy5.5, CD8-PE-Cy7 (all BD Biosciences), CD44-PE, CD25-APC, TCR β -FITC (eBioscience) and DAPI, before analysis on a FACSCanto II with FACSDiva (BD Biosciences). All samples were

analyzed with FlowJo software (Tree Star). T-cell receptor diversity was analyzed by CDR3 spectratyping as previously described [67].

Statistics

All experiments were performed at least three times. Error bars represent standard deviation (SD). Statistical significance was determined with a two-sided Student's *t*-test with unequal variance.

Accession numbers

The National Center for Biotechnology Information (NCBI) Nucleotide database (<http://www.ncbi.nlm.nih.gov/nucleotide>) accession number for the ZFN target site in intron 84 of the *prkdc* gene on mouse chromosome 16 is AB030754: 189732.

Supporting Information

S1 Table. Off-target site analysis.

(DOCX)

S2 Table. Sequences of primers used for characterization of gene targeted cells.

(DOCX)

S1 Text. Supplementary Methods.

(DOCX)

S1 Fig. ZFNs targeting *prkdc* locus. (A) Schematic view of ZFN binding site (ZFN BS) in *prkdc*. The position and sequence of the ZFN BS in intron 84 is shown. F1, F2, F3 indicate target triplets for each binding half-sites. The spacer is highlighted in italics, mut* indicates the position of the SCID mutation. (B) Sequence of *prkdc*-specific ZF modules. Amino acid sequences of the ZF modules that recognize F1, F2, or F3 target triplets for the left and right target half-sites (5' to 3' orientation). Three ZFs for the left binding half-site (L1, L2, L3) and two for the right target half-site (R1, R2) have been selected and tested for their ability to activate a beta-galactosidase (β gal) reporter [32]. (C) Expression analysis of ZFNs. ZFN-encoding plasmids were transfected in 293T cells and protein levels detected by immunoblotting using Odyssey IRDye antibodies. L1, L2, L3, ZFN left subunits 1, 2 or 3 with WT *FokI* domain; L1H, L2H, L3H, ZFN left subunits 1, 2 or 3 with "EA" obligate heterodimeric *FokI* domain [55]; L2N, ZFN left subunit L2 with "EA" obligate heterodimeric *FokI* domain without NLS signal; R1, R2, ZFN right subunits 1 or 2 with WT *FokI* domain; R1H, R2H, ZFN right subunits 1 or 2 with "QK" obligate heterodimeric *FokI* domain [55]; R1N, R2N, ZFN right subunits 1 or 2 with "QK" obligate heterodimeric *FokI* domain without NLS signal. GFP served as transfection and loading control. (D) *In vitro* cleavage assay. ZFN pair L2N and R1N was *in vitro* transcribed/translated and mixed with a ZFN BS-containing PCR product. Cleavage reaction [61] was analyzed on a 1.5% agarose gel. Size markers are indicated. (E) Plasmid-based gene correction assay. 293T cells were transfected with target plasmid, repair matrix and ZFN or *SceI* plasmids in order to induce episomal homology-directed repair [59]. Y axis shows the percentage of relative gene correction frequency, which is calculated as GFP-positive cells (target plasmid corrected) REX-positive cells (transfected cells). (+), positive control *SceI*; (-), negative control *SceI* Δ ; WT, L2 + R1 with homodimeric *FokI* domain; OH, L2 + R1 with obligate heterodimeric *FokI* domain; -NLS, L2 + R1 with OH *FokI* domain without NLS signal.

(TIF)

S2 Fig. Cellular characterization of iPSC clones. (A) Ssea-1 expression. Surface expression of pluripotency marker Ssea-1 was measured by flow cytometry. Fib.S, NOD.SCID-derived ear fibroblasts; ES.CCE, murine ES cell line; iPS.S1, iPS.S6 and iPS.S12, NOD.SCID-derived iPSC clones. (B) Alkaline phosphatase staining. NOD.SCID-derived iPSCs were stained using the Alkaline Phosphatase Detection Kit and analyzed by microscopy. (C) Spectral karyotyping (SKY). Multicolor fluorescent *in situ* hybridization (FISH) based karyotyping was used to assess genome integrity. iPS.T8 and iPS.T44, gene targeted iPSC clones. (D) Teratoma Assay. Hematoxylin/eosin-stained sections of teratoma isolated 8 weeks after injection of iPSCs into NSG mice. Detection of ectodermal, endodermal and mesodermal tissues. iPS.T8 and iPS.T44, gene targeted iPSC clones. (TIF)

S3 Fig. Molecular characterization of iPSC clones. (A) Excision of the reprogramming cassette. iPSCs have been treated with F1p recombinase to remove the lentiviral reprogramming cassette. Excision was confirmed by detection of the viral PRE elements via Southern blot. Genomic DNA was digested with *EcoRV* or *BamHI*. Positions of restriction sites in reprogramming cassette and the expected minimal band sizes are indicated on top. M, DNA size marker; S6 and S6X, SCID iPSC clones; T25 and T25X, targeted iPSC clones; WT and WTX, wild-type iPSC clones; X indicates clones with excised reprogramming cassette. (B) Random integration of donor. The *NeoR* cassette, as an indicator of donor DNA, was detected by Southern blot to confirm targeted integration in *prkdc* intron 84. Genomic DNA was digested with *EcoRV* or *NdeI*. Positions of restriction sites in the modified intron 84 and the expected band sizes are indicated on top. (C) Determination of vector copy number (VCN). Copy number of the lentiviral reprogramming vector was assessed by quantitative PCR [62], and is indicated as PRE per endogenous Flk3 copy. Fib, murine ear fibroblasts; iPS.1X and iPS.2X, iPSC clones with excised reprogramming cassette; iPS.S1, iPS.S2, iPS.S3, iPS.S4, iPS.S6, iPS.S8, iPS.S9 and iPS.S12, NOD.SCID-derived iPSC clones. (TIF)

S4 Fig. Control of *in vitro* differentiation. Samples were stained with CD41-PE, cKit-APC or their corresponding isotype controls, and 7-AAD after dissociation of 8 d matured embryoid bodies (EBs). All plots were pre-gated on FSC/SSC and 7-AAD-negativity. Red numbers indicate percentage of cells in each quadrant. iPS.WT and iPS.WT X, wild-type iPSC clones; iPS.S6 and iPS.S6 X, SCID iPSC clones; iPS.T25, iPS.T25X and iPS.T44, targeted iPSC clones; X indicates iPSC clones with excised reprogramming cassette. (TIF)

S5 Fig. Analysis of T cell receptor diversity of *in vitro* generated T cells by spectratyping. Quantitative PCR was performed on genomic DNA isolated from *in vitro* generated T cells. Exemplarily shown are PCR analyses of the variable beta chains V β 1, V β 6, V β 8.1, V β 8.3, V β 10, V β 12, V β 14 and V β 20. X axis indicates PCR fragment size in bp, Y axis shows quantity of PCR amplicons. Thymus, control DNA of cells isolated from thymus; HSC, *in vitro* generated T cells; iPS.WTX, wild-type iPSC clone; iPS.S6 and iPS.S6X, SCID iPSC clones; iPS.T25, iPS.T25X and iPS.T44, targeted iPSC clones; X indicates clones with excised reprogramming cassette. (TIF)

Acknowledgments

We thank Fabienne Lütge and Jessica Wenzl for technical support, Masumi Abe and Stephan Weger for plasmids, Juan Carlos Zúñiga-Pflücker for cells, and Nasreen Hoque, Andreas

Krüger, Nico Lachmann, Dietrich Lesinski, Ute Modlich and Bernd Schiedlmeier for experimental advice and critical discussions.

Author Contributions

Conceived and designed the experiments: SHR JK CM JKJ AS TCat. Performed the experiments: SHR JK HR CRe TM JA PF MLM TCan CRu. Analyzed the data: SHR JK HR CRe TM JA PF MLM TCan CRu CM JKJ AS TCat. Wrote the paper: SHR JK TCat.

References

1. Park IH, Arora N, Huo H, Maherali N, Ahfeldt T, et al. (2008) Disease-specific induced pluripotent stem cells. *Cell* 134: 877–886. doi: [10.1016/j.cell.2008.07.041](https://doi.org/10.1016/j.cell.2008.07.041) PMID: [18691744](https://pubmed.ncbi.nlm.nih.gov/18691744/)
2. Merkle FT, Eggen K (2013) Modeling human disease with pluripotent stem cells: from genome association to function. *Cell Stem Cell* 12: 656–668. doi: [10.1016/j.stem.2013.05.016](https://doi.org/10.1016/j.stem.2013.05.016) PMID: [23746975](https://pubmed.ncbi.nlm.nih.gov/23746975/)
3. Cavazzana-Calvo M, Andre-Schmutz I, Fischer A (2013) Haematopoietic stem cell transplantation for SCID patients: where do we stand? *Br J Haematol* 160: 146–152. doi: [10.1111/bjh.12119](https://doi.org/10.1111/bjh.12119) PMID: [23167301](https://pubmed.ncbi.nlm.nih.gov/23167301/)
4. Slatter MA, Gennery AR (2010) Primary immunodeficiencies associated with DNA-repair disorders. *Expert Rev Mol Med* 12: e9. doi: [10.1017/S1462399410001419](https://doi.org/10.1017/S1462399410001419) PMID: [20298636](https://pubmed.ncbi.nlm.nih.gov/20298636/)
5. Komori T, Okada A, Stewart V, Alt FW (1993) Lack of N regions in antigen receptor variable region genes of TdT-deficient lymphocytes. *Science* 261: 1171–1175. PMID: [8356451](https://pubmed.ncbi.nlm.nih.gov/8356451/)
6. Harrington J, Hsieh CL, Gerton J, Bosma G, Lieber MR (1992) Analysis of the defect in DNA end joining in the murine scid mutation. *Mol Cell Biol* 12: 4758–4768. PMID: [1406659](https://pubmed.ncbi.nlm.nih.gov/1406659/)
7. Gottlieb TM, Jackson SP (1993) The DNA-dependent protein kinase: requirement for DNA ends and association with Ku antigen. *Cell* 72: 131–142. PMID: [8422676](https://pubmed.ncbi.nlm.nih.gov/8422676/)
8. Shih HY, Krangel MS (2013) Chromatin architecture, CCCTC-binding factor, and V(D)J recombination: managing long-distance relationships at antigen receptor loci. *J Immunol* 190: 4915–4921. doi: [10.4049/jimmunol.1300218](https://doi.org/10.4049/jimmunol.1300218) PMID: [23645930](https://pubmed.ncbi.nlm.nih.gov/23645930/)
9. van der Burg M, Ijspeert H, Verkaik NS, Turul T, Wiegant WW, et al. (2009) A DNA-PKcs mutation in a radiosensitive T-B- SCID patient inhibits Artemis activation and nonhomologous end-joining. *J Clin Invest* 119: 91–98. doi: [10.1172/JCI37141](https://doi.org/10.1172/JCI37141) PMID: [19075392](https://pubmed.ncbi.nlm.nih.gov/19075392/)
10. Takahashi K, Yamanaka S (2006) Induction of pluripotent stem cells from mouse embryonic and adult fibroblast cultures by defined factors. *Cell* 126: 663–676. PMID: [16904174](https://pubmed.ncbi.nlm.nih.gov/16904174/)
11. Takahashi K, Tanabe K, Ohnuki M, Narita M, Ichisaka T, et al. (2007) Induction of pluripotent stem cells from adult human fibroblasts by defined factors. *Cell* 131: 861–872. PMID: [18035408](https://pubmed.ncbi.nlm.nih.gov/18035408/)
12. Garate Z, Davis BR, Quintana-Bustamante O, Segovia JC (2013) New frontier in regenerative medicine: site-specific gene correction in patient-specific induced pluripotent stem cells. *Hum Gene Ther* 24: 571–583. doi: [10.1089/hum.2012.251](https://doi.org/10.1089/hum.2012.251) PMID: [23675640](https://pubmed.ncbi.nlm.nih.gov/23675640/)
13. Choi KD, Yu J, Smuga-Otto K, Salvaggio G, Rehrauer W, et al. (2009) Hematopoietic and endothelial differentiation of human induced pluripotent stem cells. *Stem Cells* 27: 559–567. doi: [10.1634/stemcells.2008-0922](https://doi.org/10.1634/stemcells.2008-0922) PMID: [19259936](https://pubmed.ncbi.nlm.nih.gov/19259936/)
14. Irion S, Clarke RL, Luche H, Kim I, Morrison SJ, et al. (2010) Temporal specification of blood progenitors from mouse embryonic stem cells and induced pluripotent stem cells. *Development* 137: 2829–2839. doi: [10.1242/dev.042119](https://doi.org/10.1242/dev.042119) PMID: [20659975](https://pubmed.ncbi.nlm.nih.gov/20659975/)
15. Zou J, Sweeney CL, Chou BK, Choi U, Pan J, et al. (2011) Oxidase-deficient neutrophils from X-linked chronic granulomatous disease iPS cells: functional correction by zinc finger nuclease-mediated safe harbor targeting. *Blood* 117: 5561–5572. doi: [10.1182/blood-2010-12-328161](https://doi.org/10.1182/blood-2010-12-328161) PMID: [21411759](https://pubmed.ncbi.nlm.nih.gov/21411759/)
16. Zou J, Mali P, Huang X, Doney SN, Cheng L (2011) Site-specific gene correction of a point mutation in human iPS cells derived from an adult patient with sickle cell disease. *Blood* 118: 4599–4608. doi: [10.1182/blood-2011-02-335554](https://doi.org/10.1182/blood-2011-02-335554) PMID: [21881051](https://pubmed.ncbi.nlm.nih.gov/21881051/)
17. Tolar J, Park IH, Xia L, Lees CJ, Peacock B, et al. (2011) Hematopoietic differentiation of induced pluripotent stem cells from patients with mucopolysaccharidosis type I (Hurler syndrome). *Blood* 117: 839–847. doi: [10.1182/blood-2010-05-287607](https://doi.org/10.1182/blood-2010-05-287607) PMID: [21037085](https://pubmed.ncbi.nlm.nih.gov/21037085/)
18. Kennedy M, Awong G, Sturgeon CM, Ditadi A, LaMotte-Mohs R, et al. (2012) T lymphocyte potential marks the emergence of definitive hematopoietic progenitors in human pluripotent stem cell differentiation cultures. *Cell Rep* 2: 1722–1735. doi: [10.1016/j.celrep.2012.11.003](https://doi.org/10.1016/j.celrep.2012.11.003) PMID: [23219550](https://pubmed.ncbi.nlm.nih.gov/23219550/)

19. Themeli M, Kloss CC, Ciriello G, Fedorov VD, Perna F, et al. (2013) Generation of tumor-targeted human T lymphocytes from induced pluripotent stem cells for cancer therapy. *Nat Biotechnol* 31: 928–933. doi: [10.1038/nbt.2678](https://doi.org/10.1038/nbt.2678) PMID: [23934177](https://pubmed.ncbi.nlm.nih.gov/23934177/)
20. Lachmann N, Happle C, Ackermann M, Luttge D, Wetzke M, et al. (2014) Gene correction of human induced pluripotent stem cells repairs the cellular phenotype in pulmonary alveolar proteinosis. *Am J Respir Crit Care Med* 189: 167–182. doi: [10.1164/rccm.201306-1012OC](https://doi.org/10.1164/rccm.201306-1012OC) PMID: [24279725](https://pubmed.ncbi.nlm.nih.gov/24279725/)
21. Liu GH, Suzuki K, Li M, Qu J, Montserrat N, et al. (2014) Modelling Fanconi anemia pathogenesis and therapeutics using integration-free patient-derived iPSCs. *Nat Commun* 5: 4330. doi: [10.1038/ncomms5330](https://doi.org/10.1038/ncomms5330) PMID: [24999918](https://pubmed.ncbi.nlm.nih.gov/24999918/)
22. Amabile G, Welner RS, Nombela-Arrieta C, D'Alise AM, Di Ruscio A, et al. (2013) In vivo generation of transplantable human hematopoietic cells from induced pluripotent stem cells. *Blood* 121: 1255–1264. doi: [10.1182/blood-2012-06-434407](https://doi.org/10.1182/blood-2012-06-434407) PMID: [23212524](https://pubmed.ncbi.nlm.nih.gov/23212524/)
23. Suzuki N, Yamazaki S, Yamaguchi T, Okabe M, Masaki H, et al. (2013) Generation of engraftable hematopoietic stem cells from induced pluripotent stem cells by way of teratoma formation. *Mol Ther* 21: 1424–1431. doi: [10.1038/mt.2013.71](https://doi.org/10.1038/mt.2013.71) PMID: [23670574](https://pubmed.ncbi.nlm.nih.gov/23670574/)
24. Schmitt TM, Zuniga-Pflucker JC (2002) Induction of T cell development from hematopoietic progenitor cells by delta-like-1 in vitro. *Immunity* 17: 749–756. PMID: [12479821](https://pubmed.ncbi.nlm.nih.gov/12479821/)
25. Schmitt TM, de Pooter RF, Gronski MA, Cho SK, Ohashi PS, et al. (2004) Induction of T cell development and establishment of T cell competence from embryonic stem cells differentiated in vitro. *Nat Immunol* 5: 410–417. PMID: [15034575](https://pubmed.ncbi.nlm.nih.gov/15034575/)
26. Silva G, Poirot L, Galetto R, Smith J, Montoya G, et al. (2011) Meganucleases and other tools for targeted genome engineering: perspectives and challenges for gene therapy. *Curr Gene Ther* 11: 11–27. PMID: [21182466](https://pubmed.ncbi.nlm.nih.gov/21182466/)
27. Rahman SH, Maeder ML, Joung JK, Cathomen T (2011) Zinc-finger nucleases for somatic gene therapy: the next frontier. *Hum Gene Ther* 22: 925–933. doi: [10.1089/hum.2011.087](https://doi.org/10.1089/hum.2011.087) PMID: [21631241](https://pubmed.ncbi.nlm.nih.gov/21631241/)
28. Joung JK, Sander JD (2013) TALENs: a widely applicable technology for targeted genome editing. *Nat Rev Mol Cell Biol* 14: 49–55. doi: [10.1038/nrm3486](https://doi.org/10.1038/nrm3486) PMID: [23169466](https://pubmed.ncbi.nlm.nih.gov/23169466/)
29. Jinek M, Chylinski K, Fonfara I, Hauer M, Doudna JA, et al. (2012) A programmable dual-RNA-guided DNA endonuclease in adaptive bacterial immunity. *Science* 337: 816–821. doi: [10.1126/science.1225829](https://doi.org/10.1126/science.1225829) PMID: [22745249](https://pubmed.ncbi.nlm.nih.gov/22745249/)
30. Carroll D (2011) Genome engineering with zinc-finger nucleases. *Genetics* 188: 773–782. doi: [10.1534/genetics.111.131433](https://doi.org/10.1534/genetics.111.131433) PMID: [21828278](https://pubmed.ncbi.nlm.nih.gov/21828278/)
31. Araki R, Fujimori A, Hamatani K, Mita K, Saito T, et al. (1997) Nonsense mutation at Tyr-4046 in the DNA-dependent protein kinase catalytic subunit of severe combined immune deficiency mice. *Proc Natl Acad Sci U S A* 94: 2438–2443. PMID: [9122213](https://pubmed.ncbi.nlm.nih.gov/9122213/)
32. Maeder ML, Thibodeau-Beganny S, Osiaik A, Wright DA, Anthony RM, et al. (2008) Rapid "open-source" engineering of customized zinc-finger nucleases for highly efficient gene modification. *Mol Cell* 31: 294–301. doi: [10.1016/j.molcel.2008.06.016](https://doi.org/10.1016/j.molcel.2008.06.016) PMID: [18657511](https://pubmed.ncbi.nlm.nih.gov/18657511/)
33. Shao RG, Cao CX, Zhang H, Kohn KW, Wold MS, et al. (1999) Replication-mediated DNA damage by camptothecin induces phosphorylation of RPA by DNA-dependent protein kinase and dissociates RPA:DNA-PK complexes. *EMBO J* 18: 1397–1406. PMID: [10064605](https://pubmed.ncbi.nlm.nih.gov/10064605/)
34. Biedermann KA, Sun JR, Giaccia AJ, Tosto LM, Brown JM (1991) scid mutation in mice confers hypersensitivity to ionizing radiation and a deficiency in DNA double-strand break repair. *Proc Natl Acad Sci U S A* 88: 1394–1397. PMID: [1996340](https://pubmed.ncbi.nlm.nih.gov/1996340/)
35. Warlich E, Kuehle J, Cantz T, Brugman MH, Maetzig T, et al. (2011) Lentiviral vector design and imaging approaches to visualize the early stages of cellular reprogramming. *Mol Ther* 19: 782–789. doi: [10.1038/mt.2010.314](https://doi.org/10.1038/mt.2010.314) PMID: [21285961](https://pubmed.ncbi.nlm.nih.gov/21285961/)
36. Molina-Estevéz FJ, Lozano ML, Navarro S, Torres Y, Grabundzija I, et al. (2013) Brief report: impaired cell reprogramming in nonhomologous end joining deficient cells. *Stem Cells* 31: 1726–1730. doi: [10.1002/stem.1406](https://doi.org/10.1002/stem.1406) PMID: [23630174](https://pubmed.ncbi.nlm.nih.gov/23630174/)
37. Muller LU, Milsom MD, Harris CE, Vyas R, Brumme KM, et al. (2012) Overcoming reprogramming resistance of Fanconi anemia cells. *Blood* 119: 5449–5457. doi: [10.1182/blood-2012-02-408674](https://doi.org/10.1182/blood-2012-02-408674) PMID: [22371882](https://pubmed.ncbi.nlm.nih.gov/22371882/)
38. Maherali N, Hochedlinger K (2009) Tgfbeta signal inhibition cooperates in the induction of iPSCs and replaces Sox2 and cMyc. *Curr Biol* 19: 1718–1723. doi: [10.1016/j.cub.2009.08.025](https://doi.org/10.1016/j.cub.2009.08.025) PMID: [19765992](https://pubmed.ncbi.nlm.nih.gov/19765992/)
39. Hanna J, Markoulaki S, Mitalipova M, Cheng AW, Cassady JP, et al. (2009) Metastable pluripotent states in NOD-mouse-derived ESCs. *Cell Stem Cell* 4: 513–524. doi: [10.1016/j.stem.2009.04.015](https://doi.org/10.1016/j.stem.2009.04.015) PMID: [19427283](https://pubmed.ncbi.nlm.nih.gov/19427283/)

40. Voelkel C, Galla M, Maetzig T, Warlich E, Kuehle J, et al. (2010) Protein transduction from retroviral Gag precursors. *Proc Natl Acad Sci U S A* 107: 7805–7810. doi: [10.1073/pnas.0914517107](https://doi.org/10.1073/pnas.0914517107) PMID: [20385817](https://pubmed.ncbi.nlm.nih.gov/20385817/)
41. Kienker LJ, Shin EK, Meek K (2000) Both V(D)J recombination and radioresistance require DNA-PK kinase activity, though minimal levels suffice for V(D)J recombination. *Nucleic Acids Res* 28: 2752–2761. PMID: [10908332](https://pubmed.ncbi.nlm.nih.gov/10908332/)
42. van der Burg M, van Veelen LR, Verkaik NS, Wiegant WW, Hartwig NG, et al. (2006) A new type of radiosensitive T-B-NK+ severe combined immunodeficiency caused by a LIG4 mutation. *J Clin Invest* 116: 137–145. PMID: [16357942](https://pubmed.ncbi.nlm.nih.gov/16357942/)
43. Moshous D, Callebaut I, de Chasseval R, Corneo B, Cavazzana-Calvo M, et al. (2001) Artemis, a novel DNA double-strand break repair/V(D)J recombination protein, is mutated in human severe combined immune deficiency. *Cell* 105: 177–186. PMID: [11336668](https://pubmed.ncbi.nlm.nih.gov/11336668/)
44. Cagdas D, Ozgur TT, Asal GT, Revy P, De Villartay JP, et al. (2012) Two SCID cases with Cernunnos-XLF deficiency successfully treated by hematopoietic stem cell transplantation. *Pediatr Transplant* 16: E167–171. doi: [10.1111/j.1399-3046.2011.01491.x](https://doi.org/10.1111/j.1399-3046.2011.01491.x) PMID: [21535335](https://pubmed.ncbi.nlm.nih.gov/21535335/)
45. Soldner F, Laganieri J, Cheng AW, Hockemeyer D, Gao Q, et al. (2011) Generation of isogenic pluripotent stem cells differing exclusively at two early onset Parkinson point mutations. *Cell* 146: 318–331. doi: [10.1016/j.cell.2011.06.019](https://doi.org/10.1016/j.cell.2011.06.019) PMID: [21757228](https://pubmed.ncbi.nlm.nih.gov/21757228/)
46. Wang Y, Zheng CG, Jiang Y, Zhang J, Chen J, et al. (2012) Genetic correction of beta-thalassemia patient-specific iPSCs and its use in improving hemoglobin production in irradiated SCID mice. *Cell Res* 22: 637–648. doi: [10.1038/cr.2012.23](https://doi.org/10.1038/cr.2012.23) PMID: [22310243](https://pubmed.ncbi.nlm.nih.gov/22310243/)
47. Morishima T, Watanabe K, Niwa A, Hirai H, Saida S, et al. (2014) Genetic correction of HAX1 in induced pluripotent stem cells from a patient with severe congenital neutropenia improves defective granulopoiesis. *Haematologica* 99: 19–27. doi: [10.3324/haematol.2013.083873](https://doi.org/10.3324/haematol.2013.083873) PMID: [23975175](https://pubmed.ncbi.nlm.nih.gov/23975175/)
48. Lesinski DA, Heinz N, Pilat-Carotta S, Rudolph C, Jacobs R, et al. (2012) Serum- and stromal cell-free hypoxic generation of embryonic stem cell-derived hematopoietic cells in vitro, capable of multilineage repopulation of immunocompetent mice. *Stem Cells Transl Med* 1: 581–591. doi: [10.5966/sctm.2012-0020](https://doi.org/10.5966/sctm.2012-0020) PMID: [23197864](https://pubmed.ncbi.nlm.nih.gov/23197864/)
49. Holmes R, Zuniga-Pflucker JC (2009) The OP9-DL1 system: generation of T-lymphocytes from embryonic or hematopoietic stem cells in vitro. *Cold Spring Harb Protoc* 2009: pdb prot5156.
50. Reimann C, Six E, Dal-Cortivo L, Schiavo A, Appourchaux K, et al. (2012) Human T-lymphoid progenitors generated in a feeder-cell-free Delta-like-4 culture system promote T-cell reconstitution in NOD/SCID/gammac(-/-) mice. *Stem Cells* 30: 1771–1780. doi: [10.1002/stem.1145](https://doi.org/10.1002/stem.1145) PMID: [22689616](https://pubmed.ncbi.nlm.nih.gov/22689616/)
51. Gabriel R, Lombardo A, Arens A, Miller JC, Genovese P, et al. (2011) An unbiased genome-wide analysis of zinc-finger nuclease specificity. *Nat Biotechnol* 29: 816–823. doi: [10.1038/nbt.1948](https://doi.org/10.1038/nbt.1948) PMID: [21822255](https://pubmed.ncbi.nlm.nih.gov/21822255/)
52. Pattanayak V, Ramirez CL, Joung JK, Liu DR (2011) Revealing off-target cleavage specificities of zinc-finger nucleases by in vitro selection. *Nat Methods* 8: 765–770. doi: [10.1038/nmeth.1670](https://doi.org/10.1038/nmeth.1670) PMID: [21822273](https://pubmed.ncbi.nlm.nih.gov/21822273/)
53. Bibikova M, Carroll D, Segal DJ, Trautman JK, Smith J, et al. (2001) Stimulation of homologous recombination through targeted cleavage by chimeric nucleases. *Mol Cell Biol* 21: 289–297. PMID: [11113203](https://pubmed.ncbi.nlm.nih.gov/11113203/)
54. Handel EM, Alwin S, Cathomen T (2009) Expanding or restricting the target site repertoire of zinc-finger nucleases: the inter-domain linker as a major determinant of target site selectivity. *Mol Ther* 17: 104–111. doi: [10.1038/mt.2008.233](https://doi.org/10.1038/mt.2008.233) PMID: [19002164](https://pubmed.ncbi.nlm.nih.gov/19002164/)
55. Szczepek M, Brondani V, Buchel J, Serrano L, Segal DJ, et al. (2007) Structure-based redesign of the dimerization interface reduces the toxicity of zinc-finger nucleases. *Nat Biotechnol* 25: 786–793. PMID: [17603476](https://pubmed.ncbi.nlm.nih.gov/17603476/)
56. Miller JC, Holmes MC, Wang J, Guschin DY, Lee YL, et al. (2007) An improved zinc-finger nuclease architecture for highly specific genome editing. *Nat Biotechnol* 25: 778–785. PMID: [17603475](https://pubmed.ncbi.nlm.nih.gov/17603475/)
57. Porter DL, Levine BL, Kalos M, Bagg A, June CH (2011) Chimeric antigen receptor-modified T cells in chronic lymphoid leukemia. *N Engl J Med* 365: 725–733. doi: [10.1056/NEJMoa1103849](https://doi.org/10.1056/NEJMoa1103849) PMID: [21830940](https://pubmed.ncbi.nlm.nih.gov/21830940/)
58. Tebas P, Stein D, Tang WW, Frank I, Wang SQ, et al. (2014) Gene editing of CCR5 in autologous CD4 T cells of persons infected with HIV. *N Engl J Med* 370: 901–910. doi: [10.1056/NEJMoa1300662](https://doi.org/10.1056/NEJMoa1300662) PMID: [24597865](https://pubmed.ncbi.nlm.nih.gov/24597865/)
59. Alwin S, Gere MB, Guhl E, Effertz K, Barbas CF 3rd, et al. (2005) Custom zinc-finger nucleases for use in human cells. *Mol Ther* 12: 610–617. PMID: [16039907](https://pubmed.ncbi.nlm.nih.gov/16039907/)

60. Puttaraju M, DiPasquale J, Baker CC, Mitchell LG, Garcia-Blanco MA (2001) Messenger RNA repair and restoration of protein function by spliceosome-mediated RNA trans-splicing. *Mol Ther* 4: 105–114. PMID: [11482981](#)
61. Söllü C, Pars K, Cornu TI, Thibodeau-Beganny S, Maeder ML, et al. (2010) Autonomous zinc-finger nuclease pairs for targeted chromosomal deletion. *Nucleic Acids Res* 38: 8269–8276. doi: [10.1093/nar/gkq720](#) PMID: [20716517](#)
62. Kuehle J, Turan S, Cantz T, Hoffmann D, Suerth JD, et al. (2014) Modified lentiviral LTRs allow Flp recombinase-mediated cassette exchange and in vivo tracing of "factor-free" induced pluripotent stem cells. *Mol Ther* 22: 919–928. doi: [10.1038/mt.2014.4](#) PMID: [24434935](#)
63. Cathomen T, Collete D, Weitzman MD (2000) A chimeric protein containing the N terminus of the adeno-associated virus Rep protein recognizes its target site in an in vivo assay. *J Virol* 74: 2372–2382. PMID: [10666268](#)
64. Mussolino C, Alzubi J, Fine EJ, Morbitzer R, Cradick TJ, et al. (2014) TALENs facilitate targeted genome editing in human cells with high specificity and low cytotoxicity. *Nucleic Acids Res* 42: 6762–6773. doi: [10.1093/nar/gku305](#) PMID: [24792154](#)
65. Schambach A, Bohne J, Chandra S, Will E, Margison GP, et al. (2006) Equal potency of gammaretroviral and lentiviral SIN vectors for expression of O6-methylguanine-DNA methyltransferase in hematopoietic cells. *Mol Ther* 13: 391–400. PMID: [16226060](#)
66. Rudolph C, Schlegelberger B (2009) Spectral karyotyping and fluorescence in situ hybridization of murine cells. *Methods Mol Biol* 506: 453–466. doi: [10.1007/978-1-59745-409-4_30](#) PMID: [19110644](#)
67. Hechinger AK, Maas K, Durr C, Leonhardt F, Prinz G, et al. (2013) Inhibition of protein geranylgeranylation and farnesylation protects against graft-versus-host disease via effects on CD4 effector T cells. *Haematologica* 98: 31–40. doi: [10.3324/haematol.2012.065789](#) PMID: [22801964](#)